

FLUORESCENCE AND REFLECTANCE MONITORING OF HUMAN CERVICAL TISSUE *IN VIVO* A CASE STUDY

Ulf Gustafsson, Elisabeth McLaughlin, Ellen Jacobson,
Johan Håkansson, Paul Troy and Michael DeWeert
*Science and Technology International[®], 733 Bishop Street, Suite 3100,
Honolulu, Hawaii 96813, USA*

Sara Pålsson, Marcelo Soto Thompson, and Sune Svanberg
*Lund Institute of Technology, Department of Physics, P.O. Box 118,
SE-221 00 Lund, Sweden*

Aurelija Vaitkuvienė
*Vilnius University Hospital, Department of Obstetrics and Gynecology,
Antakalnio str. 57, 2040-LT, Vilnius, Lithuania*

Katarina Svanberg
*Lund University Hospital, Department of Oncology,
SE-221 85 Lund, Sweden*

ABSTRACT

An imaging spectrograph, designed and built by Science and Technology International (STI), and a point monitoring system, developed at the Lund Institute of Technology, have been used to measure the fluorescence and reflectance of cervical tissue *in vivo*. The instruments have been employed in a clinical trial in Vilnius, Lithuania, where 111 patients were examined. Patients were initially screened by Pap smear, examined by colposcopy and a tissue sampling procedure was performed. Detailed histopathological assessments were performed on the biopsies, and these assessments were correlated with spectra and images. The results of the spectroscopic investigations are illustrated by a thorough discussion of a case study for one of the patients, suggesting that the techniques are useful in the management of cervical malignancies.

Keywords: Fluorescence spectroscopy, reflectance spectroscopy, hyperspectral imaging, cervical intraepithelial neoplasia, malignancy detection.

1. Introduction

Tissue fluorescence holds great promise as a diagnostic tool for early cervical malignancy identification [1,2]. During recent years there has been a strong development in spectroscopic and imaging techniques for early detection of human malignancies. Point monitoring systems using fiber optic probes are simple but have proven efficient in many studies (see, e.g., Refs. 1-4). However, imaging spectroscopy simultaneously providing spectral information on a whole investigated scene has clear advantages in many clinical settings, and the increased complexity and cost can then be motivated. This is especially the case when the borders of the malignancies cannot easily be visualized by the naked eye, e.g. in the female outer gynecological tract, the pulmonary and ENT regions. Recent overviews of medical fluorescence imaging are given in, e.g., Refs. 5 and 6.

In the development of new diagnostic techniques, classical histopathology clearly is the gold standard to be applied for correlation with the new data. A problem in this connection is that the standard protocols only report the most severe finding of the studied region, while imaging spectroscopy might provide thousands of individual tissue spectra characterizing all parts of the investigated area. In order to correlate the fluorescence spectra with the actual biological status of the area studied, a detailed histopathological protocol was introduced [7] to provide "imaging" histopathology to match the hyperspectral images and point monitoring spectra. In this way, data from the clinical trial could be efficiently utilized.

In the particular field of gynecology, the most widely used method for initial screening for cervical intraepithelial neoplasia (CIN) and cervical cancer is a cytological smear. However, a 20 to 30 % false negative rate is associated with the Papanicolaou (Pap) smear due to insufficient sampling of cells and also to the fact that the technique is based on exfoliated cells which biological status can be misinterpreted [8]. Estimates of the sensitivity and specificity of Pap smears have been shown to range from 11 - 99% and 14 - 97%, respectively [9]. An abnormal Pap smear is normally followed by colposcopy, biopsy, histological evaluation and diagnosis. The diagnostic procedure often also includes a human papilloma virus (HPV) test for classification of the various classes of HPV. Colposcopy is performed in cases with positive results for high-risk HPV and if there is an identified lesion. The outcome of colposcopy in terms of differentiating between cervical intraepithelial lesions of various grades (CIN I-III) and inflammation/infection is highly variable and limited by operator expertise. In experienced hands, the performance average for colposcopy is sensitivity of $94 \pm 14\%$, a specificity of $51 \pm 24\%$ and a positive predictive value of $83 \pm 15\%$ [10]. In order to improve the objectivity of cervical cancer screening, tissue fluorescence spectroscopy has been suggested as a viable diagnostic aid to the physician to demarcate premalignant lesions and to guide the biopsy procedure. Different groups are currently developing suitable technology [2,4,11,12].

We have recently performed an extensive study aiming at evaluating the potential of a novel hyperspectral imaging system, which combines reflectance and fluorescence data. The investigation was supported by recordings from a point monitoring fluorescence spectroscopy device. The instruments were developed by Science and Technology International and the Lund Institute of Technology, respectively. The study was performed at the Vilnius University Hospital, Lithuania.

The clinical study provided a very large amount of useful data, which are now being fully evaluated. As a preview, a case study report is given in the present paper. A companion paper [13] gives an example of the image-processing aspects of the problem, which is greatly facilitated by the detailed histopathology and the point-monitoring fluorescence taken at a complementary excitation wavelength

2. Patients and Methods

We will describe the instrumentation used and clinical aspects of the study. First, the point monitoring and the hyperspectral systems are reviewed, followed by a description of the clinical and histopathological procedures.

2.1. Point monitoring instrument

For the point monitoring fluorescence measurements, a system developed by the Lund Institute of Technology was used [3]; see Figure 1. The emission at 337 nm from a pulsed nitrogen laser is focused into a 600 μm core diameter quartz fiber and the distal end is held in light contact to the tissue at the measurement site. The induced fluorescence is collected by the same fiber, reflected by a beam splitter into a spectrometer and captured with a gated and cooled CCD detector.



Figure 1. The point monitoring instrument in its clinical setting in Vilnius.

To obtain a high signal-to-noise ratio, the fluorescence emission from 20 laser pulses was accumulated for one spectral recording. The fluorescence background from the fiber was measured by holding the clean fiber tip in free air before the measurements and was subtracted from all spectra before storage and subsequent analysis. The optical fibers used were sterilized with 70% ethanol between the patient procedures. All spectra were spectrally corrected for the optics transmission and the uneven response from the detectors using a NIST-calibrated tungsten-halogen lamp.

2.2. Hyperspectral imaging instrument

The Hyper-Spectral Diagnostic Imaging (HSDI[®]) instrument, designed and built by Science and Technology International is a hyperspectral imaging spectrograph for early diagnosis of cervical malignancy; see Figure 2. The HSDI instrument collects both fluorescence and white light reflectance in the 400 to 760 nm region. The HSDI instrument has a spatial resolution of 230 microns at its normal working distance of 0.3 meters. The HSDI instrument includes a high-resolution digital RGB camera, which is used to collect standard colposcopic images concurrently with hyperspectral imaging. The RGB images are used as references for registering the fluorescence and reflectance, and for marking the localization of collected biopsy specimen.



Figure 2. The Hyperspectral Diagnostic Imaging instrument in the clinical setting in Vilnius.

The data collection procedure of the HSDI instrument is outlined in Figure 3. The hyperspectral sensor uses a progressive line scan to capture an entire image. Figure 3a shows the conventional colposcopic RGB image. For each scan line, the full spectrum for every pixel is provided, as indicated in Figure 3b. By taking a number of lines, a hyperspectral cube is developed, shown in Figure 3c. This hyperspectral cube contains spatial information in two dimensions and spectral information in the third dimension.

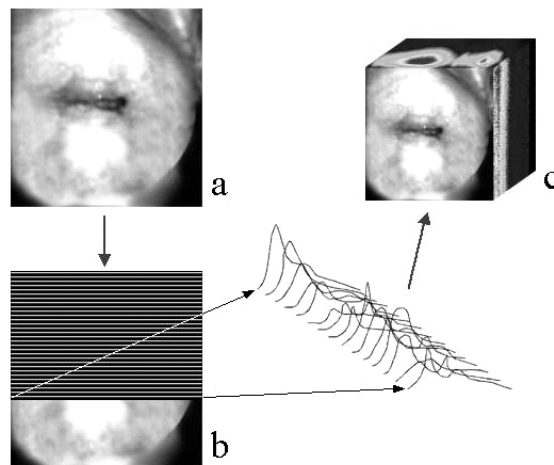


Figure 3. The line scan procedure used in the HSDI instrument. a) Conventional colposcopic image. b) Line scan with associated spectrum for each pixel. c) Resulting hyperspectral cube.

The hyperspectral cubes were spectrally and spatially corrected for the spectral and spatial non-uniformity of the optics, detectors and illumination sources using a reflectance standard and an integrating sphere, both NIST-calibrated.

2.3. Clinical set-up

The clinical study was conducted in Vilnius, Lithuania, in August and September 2001. Patients for this study consisted of postmenarchal women with indications for colposcopy. Women were recruited to undergo hyperspectral imaging and point monitoring measurements during their colposcopic examination. Inclusion criteria were females over the age of 18, indication for colposcopy or due for routine pelvic examination, no history of cervical dysplasia, and no acute diagnosis of infectious cervicovaginitis. Patients were excluded if they had a known or suspected pregnancy. One hundred eleven patients were enrolled in the study, which was approved by the Lithuanian bioethics committee.

After obtaining informed consent, the patient's demographic data and pertinent medical history were gathered. The patients were placed in the examination position and a vaginal speculum was inserted. The HSDI instrument was positioned to optimize the focus of the instrument. The cervix was first scanned in a reflectance recording with white light for approximately 10 seconds. This was followed by a fluorescence scan, requiring approximately 12 seconds. Both the fluorescence and the reflectance scans are non-contact and non-invasive. Following the two scans the cervix was cleansed with a large cotton swab soaked with a diluted solution (3-5%) of acetic acid as is standard practice in colposcopy. After application of acetic acid, the epithelium is whitened due to the dissolution of the mucus, and intracellular dehydration and coagulation of proteins. The patterns that appear, punctation, mosaic structures and atypical vessels, are identified by the gynecologist. These signs are, however, seen in both pre-cancerous lesions and various degrees of cervicitis. Therefore, the clinical challenge is to find a tool to discriminate between these conditions. A colposcopic examination of the cervix according to the standard procedure was conducted using white light illumination. The physician inspected the cervix for lesions and areas of suspicion. This was followed by "post-acetic" reflectance and fluorescence scans with the HSDI system.

Next the patient underwent fluorescence point monitoring. Unlike the reflectance and fluorescence scans, the point monitoring does make limited contact with the surface of the cervix. Up to 36 point monitoring recordings were acquired. Subsequently, iodine staining was performed. Based on the colposcopic findings, biopsies, sections, mini-, and maxi-conizations were taken using electrical loops.

2.4. Histopathology

Excised tissue samples were prepared for pathologic examination. Two independent pathologists reviewed the micrographic slides. The first pathology examination was conducted in Vilnius and the result was immediately reported to the patient and used for treatment and follow-up. A pathologist in Lund, Sweden, conducted a second pathology review. This review was performed according to a detailed histopathological protocol [7], which accounts for multiple sites and detailed morphological details potentially influencing the recorded spectrum. The orientation and location of the biopsy sites were recorded as precisely as possible on sampling. The examination allowed for a very accurate correlation between histopathology and the recorded optical signals. An example of biopsy sites and pathological information according to the new detailed protocol is shown in Figure 4.

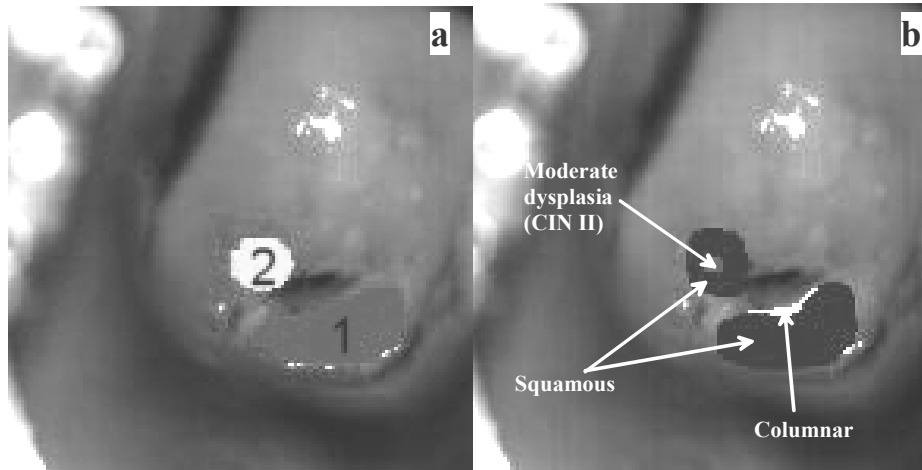


Figure 4. An example of geometrically referenced biopsy sampling (a) and classified tissue types (b).

In order to locate measurements and to correlate with pathology in point monitoring, circular co-ordinates were used on the cervix, see Figure 5. The cervix is divided into 16 "clock" numbers and as radial units, the terms squamous epithelium, transformation zone and glandular tissue were used.

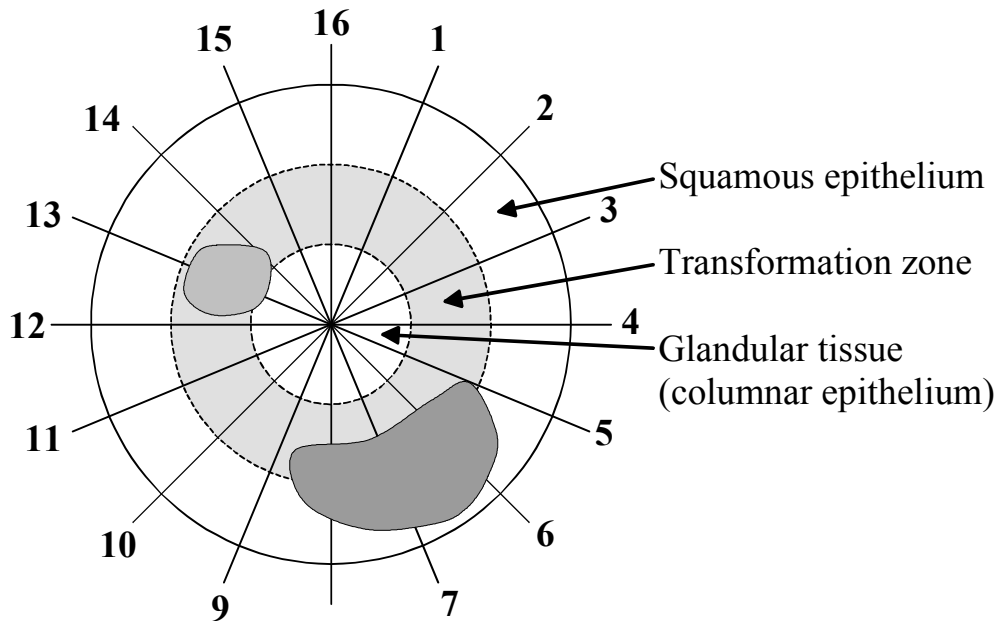


Figure 5. Circular cervical co-ordinate system used in point monitoring and for image referencing. The areas marked indicate biopsy regions.

3. Results

Using the detailed described pathology method, the opportunities are given to construct histopathology maps of the cervical area and to correlate each individual recorded spectrum with the detailed pathology evaluated in the corresponding region. A huge amount of data was gathered in the present study, now under evaluation. As an illustration of the outcome, data from one representative patient (Patient #98) exhibiting various tissue types are presented as a case study with information obtained from point monitoring as well as hyperspectral imaging.

3.1. Point monitoring

Point monitoring spectra were recorded for patient 98 as illustrated in Figure 6. A suspicious area was visually identified in the clock sectors 15 to 16 and excised after the spectral measurements. The spectra were taken radially starting at the outer border of the cervix and progressing towards the cervical channel, as indicated with star marks. Pathology revealed normal tissue in the direction 16, while a mix of low and moderate dysplasia (CIN I and CIN II) was diagnosed along direction 15. The star-marked (★) spectra in the right panel thus correspond to normal tissue and the star-marked (★) spectra in the left panel correspond to dysplasia. We note an overall intensity reduction in the dysplastic spectra, which is a common observation for malignancies (see, e.g., [14]) and a tendency of an over-all red-shift. The diamond-marked (◆) spectra in the left panel, with higher intensities and blue-shifted with respect to the star-marked (★) in the same panel, correspond to visually non-suspicious tissue, however not biopsied.

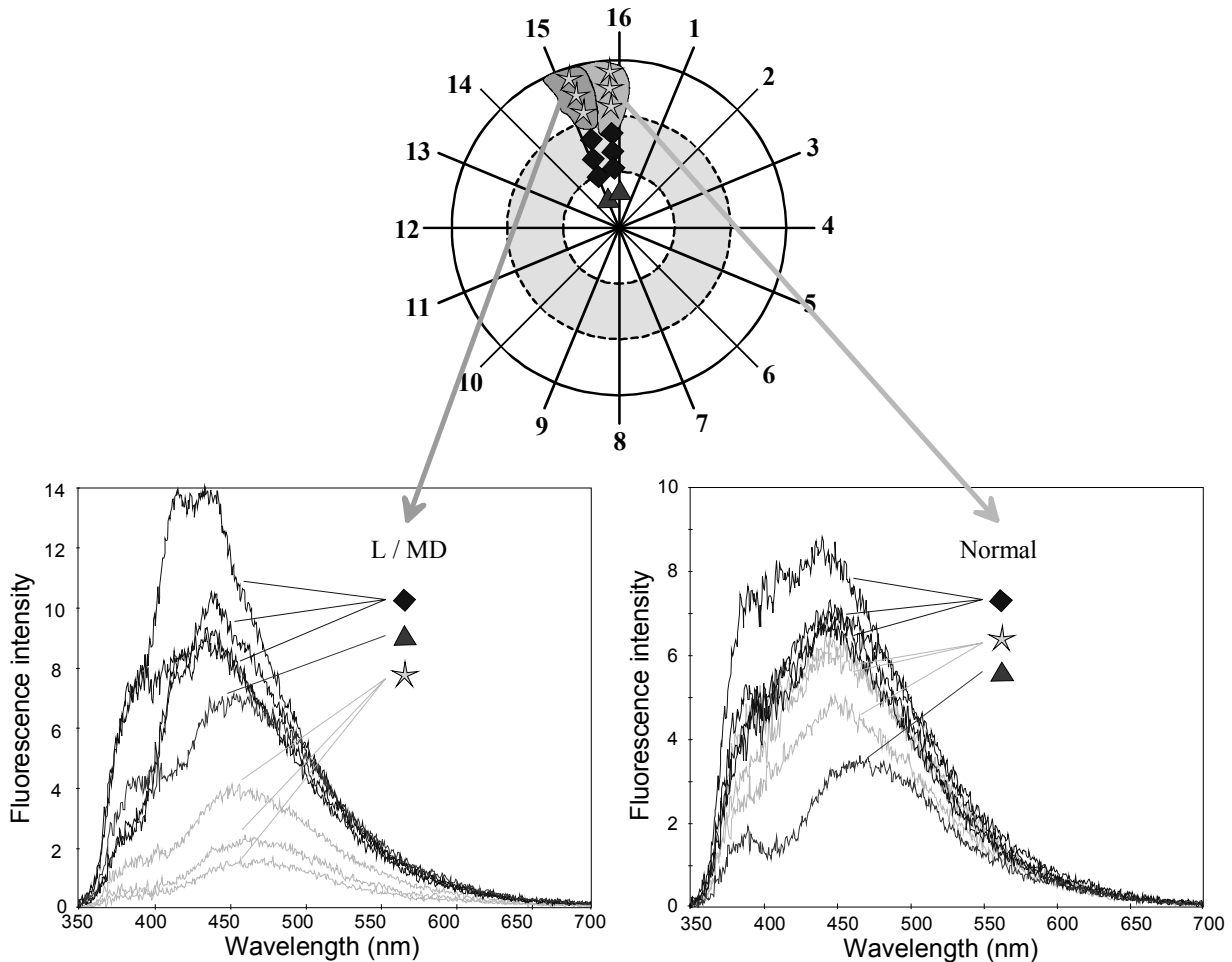


Figure 6. Point monitoring spectra from one of two biopsies from patient 98 with an illustration of the positions measured (upper). Histopathology diagnosed the leftmost region of the biopsy as low to moderate dysplasia (L/MD) and the rightmost region was diagnosed as normal.

3.2. Hyperspectral imaging

Full hyperspectral reflectance and fluorescence image cubes as well as RGB color images were acquired for patient 98. The biopsied regions were indicated on the reflectance image for correlation with the histopathological examination. The biopsy map, the RGB image and one band in the reflectance and the fluorescence hyperspectral cubes are displayed in Figure 7. The images shown are all acquired after the acetic-acid wash (post-acetic images). The reflectance and

fluorescence hyperspectral images are separated in time, by about 10-15 seconds, and in space by patient movement. As an example, a trickle of blood is observed in the reflectance image and has traveled further down the cervix in the fluorescence image, which is acquired after the reflectance image. This patient had exposed stroma, evident as red areas, and patches of blood.

The histopathological examination revealed a lesion, low to moderate grade dysplasia (CIN I and CIN II) in upper part of biopsy region 1. The position of the lesion is also illustrated in Figure 6 for the point monitoring system. Region 2 was diagnosed as normal squamous tissue. The acetic acid dissolves the mucus and accentuates atypical areas by inducing intracellular dehydration and coagulation of proteins. However, this is the same appearance for inflammation as for various grades of CIN lesions. The atypical areas are clearly visible in the reflectance images as aceto-whitened regions, especially in biopsy region 1. This region is not as obvious in the fluorescence image.

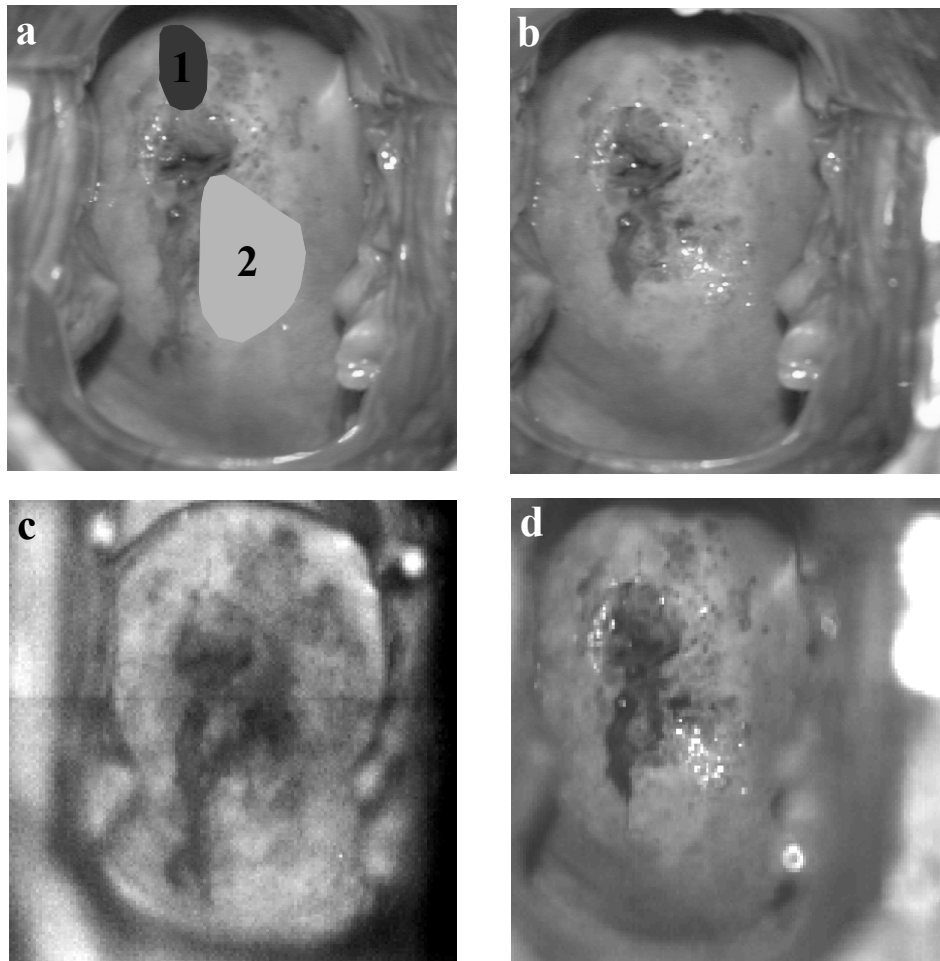


Figure 7 a) Biopsied regions. b) RGB image of the cervix. c) Fluorescence image from one wavelength band in the hyperspectral fluorescence cube. d) Reflectance image from one wavelength band in the hyperspectral reflectance cube.

A spectral analysis using Bayesian multi-variant statistics of the reflectance and the fluorescence hyperspectral images is shown in Figure 8. Detections for low to moderate grade dysplasia are localized in the region of the lesion for both reflectance and fluorescence. Detection is also visible in other, aceto-whitened, regions on the cervix. These regions were, however, not biopsied.

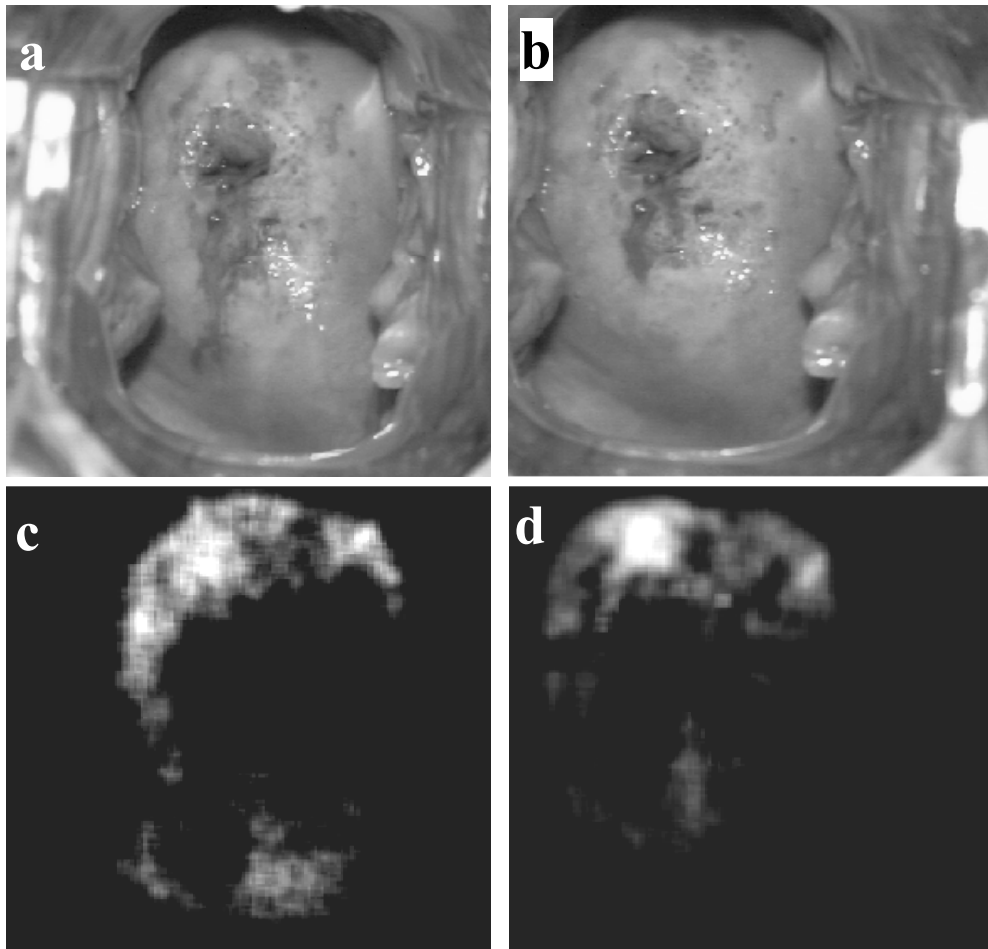


Figure 8. Spectral analysis of the reflectance and the fluorescence hyperspectral image cubes. a-b) RGB images of the cervix. c-d) Corresponding spectral detection of low/moderate grade dysplasia in fluorescence and reflectance, respectively.

4. Discussion and conclusions

We have employed a hyperspectral imaging instrument and a point monitoring system in a clinical study to evaluate the potential of the two approaches for the detection of early cervical malignancies. In this paper we have presented a case study report. The very large amount of data collected during the clinical trial is now being evaluated and will be presented in a future paper.

The analysis utilized a new detailed histopathological protocol which accounts for multiple sites and provides a detailed histopathological map within the regions biopsied. The new histopathological examination allows for a very accurate correlation between histopathology and the recorded spectral signal. This correlation is illustrated in Figure 6 for the point monitoring data, where different tissue types within one biopsy region clearly exhibit different spectral signatures. Compared to the visually non-suspicious areas, an overall intensity reduction and a red-shift are observed in the dysplastic spectra. This correlation would not be possible using the standard histopathological protocol, which only reports the most severe condition within the entire biopsy region.

The hyperspectral result is in accordance with the point monitoring result. A spectral analysis of the entire image detects, as illustrated in Figure 8, the low/moderate grade dysplastic lesion in both fluorescence and reflectance.

Suspected false alarm lesions can also be identified. These regions were, however, not biopsied, making it impossible to determine whether they are true false alarms. Histopathological information is only available within the excised tissue regions, and it is only within these regions a true correlation between the histopathological map and the spectral signatures can be made. An advantage of spectral imaging is, however, the generation of a hyperspectral image cube with a very large number of spectra available for processing. This information can be used to guide the physician to other suspicious tissue regions.

ACKNOWLEDGMENTS

The authors would like to recognize Jody Oyama and R.B. Sieple for operating the HSDI instrument during the clinical trials, and Reda Ziobakiene, Violeta Poskiene, and Kristina Kriukelyte for performing Vilnius clinical trial colposcopy examinations and biopsy sampling. The authors are further grateful to Unne Stenram for detailed histopathological work, Gary Bignami and Stefan Andersson-Engels for insightful discussions on medical spectroscopy, and Nicolas Susner and Science and Technology International for supporting this work.

REFERENCES

1. S. Andersson-Engels, Å. Elner, J. Johansson, S.-E. Karlsson, L.G. Salford, L.-G. Strömblad, K. Svanberg and S. Svanberg, Clinical recording of laser-induced fluorescence spectra for evaluation of tumour demarcation feasibility in selected clinical specialities, *Lasers Med. Sci.* **6**, 415-424 (1991).
2. M.F. Mitchell, S.B. Cantor, N. Ramanujam, G. Tortolero-Luna and R. Richards-Kortum, Fluorescence spectroscopy for diagnosis of squamous intraepithelial lesions of the cervix, *Obstet. Gynecol.* **93**, 462-470 (1999).
3. C. af Klinteberg, M. Andreasson, O. Sandström, S. Andersson-Engels and S. Svanberg, Compact medical fluorosensor for minimally invasive tissue characterisation, Submitted to Rev. Sci. Instrum. (2002).
4. R.J. Nordstrom, L. Burke, J.M. Niloff and J.F. Myrtle, Identification of cervical intraepithelial neoplasia (CIN) using UV-excited fluorescence and diffuse-reflectance tissue spectroscopy, *Lasers Surg. Med.* **29**, 118-127 (2001).
5. G.A. Wagniers, W.M. Star, and B.C. Wilson, In vivo fluorescence spectroscopy and imaging for oncological applications, *Photochem. Photobiol.* **65**, 603-632 (1998).
6. S. Andersson-Engels, K. Svanberg and S. Svanberg, Fluorescence imaging in medical diagnostics, in *Biomedical Optics*, ed. J.G. Fujimoto, to appear.
7. S. Pålsson, U. Stenram, M. Soto Thompson, A. Vaitkuviene, V. Poskiene, R. Ziobakiene, J. Oyama, N. Bendsoe, S. Andersson-Engels, S. Svanberg and K. Svanberg, Methods for detailed histopathological investigation and localisation of cervical biopsies to improve the interpretation of autofluorescence data, Manuscript in preparation (2003).
8. L.G. Koss, The Papanicolaou test for cervical cancer detection: A triumph and tragedy, *JAMA* **261**, 737-743 (1989).
9. M.T. Fahey, L. Irwig, and P. Macaskill, Metaanalysis of pap test accuracy, *Am. J. Epidemiol.* **141**, 680-689 (1995).
10. M.F. Mitchell, Accuracy of colposcopy, *Consult. Obstet. Gynecol.* **6**, 70-73 (1994).
11. I. Georgakoudi, E.E. Sheets, C.P. Crum, M.G. Muller, V. Backman and M.S. Feld, Tri-modal spectroscopy as a tool for detecting cervical squamous intraepithelial lesions in vivo, in *Diagnostic optical spectroscopy in biomedicine*, eds. T. Papazoglou and G.A. Wagnieres, Proc. SPIE vol. **4432**, 1-9 (2001).
12. C. af Klinteberg, C. Lindquist, I. Wang-Nordman, A. Vaitkuviene and K. Svanberg, Laser-induced fluorescence studies of premalignant and benign lesions in the female genital tract, in *Optical Biopsies and Microscopic Techniques II*, eds. I.J. Bigio, K. Svanberg, H. Schneckenburger, J. Slavik and P.M. Viallet, Proc. SPIE vol. **3197**, 34-40 (1997).
13. M.J. DeWeert, J. Oyama, E. McLaughlin, E. Jacobson, J. Håkansson, G.S. Bignami, U. Gustafsson, P. Troy, V. Poskiene, K. Kriukelyte, R. Ziobakiene, A. Vaitkuviene S. Pålsson, M.S. Thompson, U. Stenram, S. Andersson-

Engels, S. Svanberg, and K. Svanberg, Analysis of Spatial Variability in Hyperspectral Imagery of the Uterine Cervix In Vivo, in *Spectral Imaging: Instrumentation, Applications and Analysis*, eds. R.M. Levenson, G.H. Bearman, and A. Mahadevan-Jensen, Proc SPIE vol. **4959** (2003).

14. L. Baert, R. Berg, B. van Damme, M.A. D'Hallewin, J. Johansson, K. Svanberg and S. Svanberg, Clinical fluorescence diagnosis of human bladder carcinoma following low-dose Photofrin injection, *Urology* **41**, 322-330 (1993).